The Long Bone Histology of the Sauropodomorph, *Antetonitrus ingenipes*

EMIL KRUPANDAN[1*] **ANUSUYA CHINSAMY-TURAN**[1] **AND DIEGO POL**[2,3]

[1]Department of Biological Sciences, University of Cape Town, Private Bag X3, Rhodes Gift, 7701, South Africa

[2]Museo Paleontológico Egidio Feruglio, Av. Fontana 140, Trelew, Chubut Province, U9100GYO, Argentina

[3]Consejo Nacional de Investigaciones Científicas y Técnicas (CONICET), Av. Rivadavia 1917 (C1033AAJ), Ciudad Autónoma de Buenos Aires, República Argentina

ABSTRACT

This analysis of the long bone microstructure of *Antetonitrus ingenipes* fills a crucial gap in our understanding of the growth dynamics of sauropodomorph dinosaurs. The bone histology of basal Sauropodomorpha are often characterized by zonal tissue, and contrasts with that of more derived sauropod taxa which show a shift toward the deposition of uninterrupted fibrolamellar bone (with lines of growth being either absent or only present in the outer circumferential layer). In *Antetonitrus*, growth patterns in the youngest individuals exhibit uninterrupted fibrolamellar bone without any growth marks. Subadult individuals, also exhibit highly vascularized fibrolamellar bone throughout the cortex, as in more derived Sauropods and Mussaurus, but growth lines occur intermittently (although not regularly) throughout the cortex as in Lessemsaurus. This indicates that *Antetonitrus* does not exhibit the growth dynamics previously considered characteristic of Sauropoda. Despite this, the largest (and possibly the oldest femur, NMQR 1705/163) does show an incipient external fundamental system (EFS). Our findings further suggest that growth marks are decoupled from bone size, which indicates a level of developmental plasticity in this taxon. Modulations or textural shifts in the pattern of vascular channel arrangements throughout the fibrolamellar bone in the cortex may be related to periods of resource limitations, although the lack of consistency of these modulations suggest that it is unlikely due to seasonal fluctuations. Localized bands of radial fibrolamellar bone, followed by resumption of normal growth in two samples are interpreted as evidence of a disease infliction, and subsequent recovery thereof. Anat Rec, 301:1506–1518, 2018. © 2018 Wiley Periodicals, Inc.

Key words: *Antetonitrus*; sauropod; dinosaur; histology; bone microstructure; ontogeny

Bone microstructure (osteohistology) provides a direct record of ontogenetic growth and provides a wealth of data on various aspects of dinosaur paleobiology, such as, growth rates, ontogenetic stages, and termination of growth (e.g., Chinsamy-Turan, 2005; Cerda et al., 2013). Studies of the bone histology of sauropodomorph bones have been

Grant sponsor: The Palaeontological Scientific Trust ; Grant sponsor: National Research Foundation; Grant sponsor: Scarce Skills Bursary and Paleontological and Scientific Trust.

*Correspondence to: Emil Krupandan, Department of Biological Sciences, University of Cape Town, Private Bag X3, Rhodes Gift 7701, South Africa

E-mail: emilkrupandan@hotmail.com

Received 24 February 2017; Revised 4 February 2018; Accepted 28 February 2018.

DOI: 10.1002/ar.23898

Published online in Wiley Online Library (wileyonlinelibrary.com).

conducted on several taxa, with particularly detailed work on the basal sauropodomorphs *Massospondylus carinatus* (Chinsamy, 1993a, 1993b) and *Plateosaurus engelhardti* (Sander and Klein, 2005; Klein and Sander, 2007).

Recently the bones of sauropodiform taxa such as *Aardonyx celestae* (Yates et al., 2010), *Leonerasaurus taquetrensis* (Pol et al., 2011) and *Mussaurus patagonicus* (Cerda et al., 2014) have also been histologically examined, and have shed new light on the biology of these transitional forms *en route* to the sauropod bauplan. Although extensive studies on sauropod bone microstructure have been made over the past few years (Curry, 1999; Sander, 2000; Sander et al., 2004; Lehman and Woodward, 2008; Klein and Sander, 2008; Sander et al., 2011a; Curry Rogers et al., 2016), except for Sander et al. (2004) all of these studies have focused on neosauropod taxa.

The first (ostensibly) basal sauropod to be studied histologically is that of an unnamed taxon from the Norian-Rhaetian aged Nam Phong Formation of Thailand (Buffetaut et al., 2002; Sander et al., 2004). Based on its size (comparable to that of *Apatosaurus louisae*) and location 1 km away from the *Isanosaurus attavipachi* holotype site, it is possible that the remains pertain either to an adult specimen of *Isanosaurus* or to another unknown sauropod taxon (Buffetaut et al., 2002; Sander et al., 2004). Sander et al. (2004) found that this sauropod had uninterrupted laminar fibro-lamellar bone, which characterizes later Jurassic sauropods (Sander et al., 2004, 2011a). At the time of publication, *Isanosaurus* and the conferred material (see Sander et al., 2011a) represented the earliest sauropod remains discovered. Although the conferred material was found nearby, in the same formation, poor preservation and lack of skeletal element overlap with the holotype of *Isanosaurus*, prevents an actual diagnosis beyond Sauropoda indet (Buffetaut et al., 2000, 2002).

Bone histology studies of ontogenetic series of the basal sauropodomorph *Massospondylus carinatus* (Chinsamy, 1993a, 1993b; Chinsamy-Turan, 2005) and *Plateosaurus engelhardti* (Sander and Klein, 2005; Klein and Sander, 2007; Hurum et al., 2006) show that basal sauropodomorphs are characterized by zonal bone (*sensu* Reid, 1981) which is composed of fibrolamellar bone (FLB) tissue interrupted by growth marks (Lines of Arrested Growth [LAGs] or annuli). In the case of *Plateosaurus*, termination of growth is recorded in the subperiosteal margin (Klein and Sander, 2007), while even the largest individual of *Massospondylus* does not show the closely spaced rest lines indicative of attainment of skeletal maturity (Cerda et al., 2017). Extensive studies of *Plateosaurus* have shown a marked degree of developmental plasticity (Sander and Klein, 2005), indicated by different sized elements possessing similar numbers of growth rings.

Based on samples taken from the scapula and rib, the sauropodiform taxon, *Aardonyx* appears to exhibit cortical bone tissue that is zonal and similar to that of the basal sauropodomorphs (Yates et al., 2010). The rib histology of *Leonerasaurus* also has zonal bone tissue (Pol et al., 2011), although the fibrolamellar bone is less vascularized in this taxon.

Recent studies on *Mussaurus* showed that it had a faster growth rate than *Massospondylus* [Cerda et al., 2014], with a much higher proportion of vascularization, as compared to *Aardonyx* and *Leonerasaurus*. Furthermore, the pattern of vascularization varies between laminar, plexiform and reticular FLB (Cerda et al., 2014). The lack of growth lines in juvenile *Mussaurus* material indicates a phase of rapid continuous growth during early ontogeny, similar to that experienced by sauropods throughout most of their lives. In adult *Mussaurus* individuals, there is evidence of the presence of growth marks restricted to the outer third of the of the cortex (Cerda et al., 2014, Cerda et al., 2017). Thus, it appears that *Mussaurus* possesses the "typical" sauropod growth pattern (see below); however, Cerda et al. (2017) ascribe this to homoplasy rather than being a synapomorphic character for basal Sauropodomorpha and Sauropoda based on the results of character optimization.

In contrast to the more basal sauropodomorphs, sauropods appear to have a highly vascularized fibrolamellar bone tissue, with LAGs being scarce and only occurring toward the subperiosteal margin (referred to as an external fundamental system by Klein and Sander [2008] or outer circumferential lamella by Chinsamy-Turan [2005]), indicating rapid uninterrupted growth followed by a slowing down in deposition rates (Sander et al., 2004; Chinsamy-Turan 2005; Sander et al., 2011a, 2011b). However, it should be noted that there are exceptions to this trend. Based on material now identifiable as belonging to the titanosauriform *Lapparentosaurus* (De Ricqlès, 1983; Rimblot-Baly et al., 1995; Sander, 2000; Mannion, 2010), BMNH R9472—an undescribed Middle Jurassic sauropod (Reid, 1981), *Europasaurus* and *Lessemsaurus* (Cerda et al., 2017), there is clear evidence of cyclical growth marks in the inner cortex of sauropod bones. As early as 1983, De Ricqlès pointed out that these cyclical growth rates may be more prevalent in sauropods than previously thought.

Antetonitrus ingenipes (Yates and Kitching, 2003) from the Norian, Lower Elliot Formation of South Africa is geologically older than the Thai basal sauropod, and according to recent phylogenetic analyses (Apaldetti et al., 2013; Otero and Pol, 2013; McPhee et al., 2014) is even more basal than *Isanosaurus*. Thus, *Antetonitrus* is now considered to be the earliest sauropod (Yates, 2007).

In addition to the holotype material (BPI/1/4952), the same unique combination of characters and autapomorphies (indicated with *) for *Antetonitrus*, identified by Yates and Kitching (2003) and expanded on by McPhee et al. (2014), are present in NMQR 1705—and are the basis for referring this material to this taxon (Krupandan personal observation, 2017): dorsal neural spines flared transversely at their distal end*; dorsal vertebrae with broad, triangular hyposphenes (in caudal view)*; an extremely short, broad metacarpal I* and a deep sulcus adjacent to the lateral distal margin of the deltopectoral crest*; high dorsal neural spines comprising more than half the total height of the neural arch*; a single articular facet on the proximal chevrons*; the head of the humerus is vaulted and expanded posteriorly; the medial tuberosity of the humeral head is reduced and slightly medially inturned*; a medial deflection of the anterior process of the proximal ulna*; an incipient radial fossa on the proximal ulna; a distinct bifurcated tubercle on the ventrolateral edge of the shaft of the second metacarpal; the femoral shaft is elliptical in cross-section and reduced in lateral sinuosity; the fourth trochanter is located on the medial edge of the mid-shaft of the femur; the anteroposterior length of the proximal surface of the tibia is over twice its transverse width and roughly level with the horizontal plane; the descending process of the distal tibia is compressed laterally so that the anterior ascending

process is visible in posterior view; and a robust, entaxonically spreading pes. The hyposphenes of the caudal vertebrae are not preserved, precluding determination of whether NMQR 1705 also possessed a ventral ridge on the caudal hyposphenes.

Here, we undertake an osteohistological study of *Antetonitrus* (BPI/1/4952 and NMQR 1705) to assess whether it had a growth strategy more similar to basal sauropodomorphs, or to its more derived relatives or whether instead it exhibited a completely different growth. Furthermore, we studied different sized femora, tibia and humeri to deduce histological variation in long bone histology, and to assess how they grew through ontogeny.

Institutional Abbreviations

BMNH, British Museum of Natural History; BPI, Evolutionary Studies Institute, Johannesburg, South Africa; NMQR, National Museum, Bloemfontein, South Africa.

MATERIALS AND METHODS

Samples were taken from the long bone elements (femora, humeri, and tibiae) of NMQR 1705, a mono-specific, multi-individual assemblage collected from the Late Triassic, Lower Elliot Formation (LEF) site of Maphutseng, Lesotho (Ellenberger and Ellenberger, 1956; Charig et al., 1965; Gauffre, 1993; Bordy et al., 2015; Krupandan personal observation, 2014). In addition to this, a core from the femur of the holotype (BPI/1/4952) was also included. No data on association between elements for NMQR 1705 was available as this material was excavated during the 1950s and accessioned at NMQR as disarticulated material without any field notes. While some NMQR 1705 elements clearly articulate with each other (e.g., pedal phalanges), it cannot be accurately determined whether the long bones sampled belong to the same individuals as the only way to associate material would be based on ratios taken from the holotypic material (BPI/1/4952)—the results of which are equivocal at best due to some elements being incomplete.

Samples were taken from the femoral, tibial, and humeral midshaft regions (identified by Chinsamy [1993b] and Klein and Sander [2007] as being neutral regions of growth with the least remodeling). To ensure that the best possible record of growth was analyzed, full cross-sections were sampled of the femora and tibia to determine the best region for core sampling (Stein and Sander, 2009). Due to the poor preservation of the humeri, only one was cored, partial segments of the bone wall of the other two were sampled. As far as possible, cores were taken from comparable regions. Specimens were cored using a drill with a diamond encrusted coring bit or cut using a Dremel Precision Tool. After samples were removed from the bone the area was infilled with plaster to retain the original shape of the bone. In the case of full cross-sections, casts of the removed slices were made with epoxy and inserted into the missing regions of the bones.

Eight femora (NMQR 1705/252, 1705/20, 1705/801, 1705/163, 1705/325, 1705/15, 1705/600, and BPI/1/4952) representing a size range of 435 mm to 885 mm in length were sampled. A thin section of the complete cross-section of the bone wall of NMQR 1705/163 permitted the determination that the posteromedial side of the midshaft was the thickest part of the bone wall and therefore held the best record of ontogenetic growth. All other femora were cored in this region. The exception to this was that the holotype femur (BPI/1/4952) was sampled from the posterior side of the distal femur, just proximal to the lateral and medial condyles, this core was taken before rules governing destructive sampling of South African holotypic material came into effect and subsequently no further sampling was permitted.

Six tibiae ranging in size from 322 mm to 565 mm in length were sampled for histological analyses. A complete cross-section of tibia NMQR 1705/235 indicated that the best location for core sampling was from the anteromedial or posterior sides of the midshaft of the tibia. The remaining five tibiae were sampled (1705/304, 1705/561, 1705/100, 1705/354, and 1705/009) in this region. Three humeri (NMQR 1705/801, 1705/028, and 1705/359), ranging in size from 570 mm to 620 mm in length were sampled in the anterolateral half of the midshaft.

Specimens were prepared for thin sections based on the methodology outlined in Chinsamy and Raath (1992). Cores/samples were embedded in resin (Struers Epofix), mounted on frosted glass slides and thin-sectioned using a Struers Accutom-50. The preparation of the histological sections was carried out at the University of Cape Town, South Africa. All sections were studied using a Nikon E200 microscope. Photomicrographs were captured using NIS D 3.0 Software and edited in Adobe Photoshop CC 2014. Nomenclature and definitions of structures used in this study are *sensu* Chinsamy-Turan (2005).

Comparative material includes published data on the following basal sauropodomorphs; *Massospondylus* (Chinsamy, 1993b, 1994), *Plateosaurus* (Sander and Klein, 2005; Klein and Sander, 2007), and the basal sauropodiforms, *Aardonyx* (Yates et al., 2010), *Leonerasaurus* (Pol et al., 2011), and *Mussaurus* (Cerda et al., 2014, 2017). BMNH R9472 (Reid, 1981), *Lapparentosaurus* (see De Ricqlès, 1983, Rimblot-Baly et al., 1995, Mannion 2010), the Nam Phong sauropod (Sander et al., 2004), *Apatosaurus* (Curry, 1999), and the Tendaguru sauropods (Sander, 2000) were used as examples of derived Sauropoda.

RESULTS

Detailed Histology of the Femora

All eight midshaft femoral samples exhibit well-vascularized, primary FLB tissue throughout the cortex. The vascular organization of the FLB is generally characterized by an irregular, reticular arrangement of the vascular channels in the inner-most cortex and a change in arrangement of the channels to a plexiform (composed of radial and circumferential channels) arrangement in the subperiosteal cortex. Secondary osteons are present in all femora, except the smallest—NMQR/1705/252 (435-mm length). While NMQR/1705/020 (756-mm length) shows the change from reticular to plexiform FLB seen in most of the sampled bones, a thin band of avascular tissue (? annulus) is evident below the three LAGs that are present near the outer region of the cortex (Fig. 1). In contrast to this general pattern, NMQR/1705/801 (760-mm length) exhibits only reticular FLB, except for a small patch of plexiform tissue in middle of the cortex (Fig. 2).

NMQR/1705/163 (Fig. 3), the 5th largest femur (770-mm length), shows a four stage change in vascular orientation from outer cortex to the medullary region: in the outermost region there is a thin layer of less

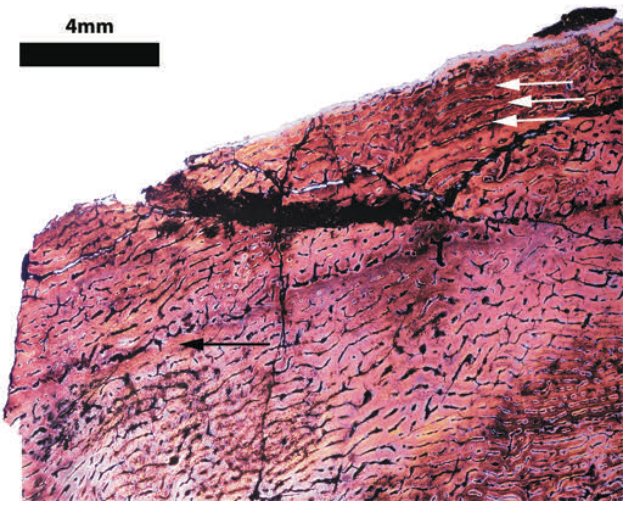

Fig. 1. Right femur, NMQR 1705/020. Polarized light. Black arrow indicates thin band of avascular tissue/annulus. White arrows show LAGs.

vascularized FLB with a vascular organization composed of a combination of plexiform tissue, but with significant number of irregular channels as well (Fig. 3B), below which is a thicker region of less organized reticular FLB (Fig. 3C), followed by a thinner layer of plexiform tissue (Fig. 3D), which overlies reticular FLB (with large amounts of secondary osteons) that occurs throughout the rest of the compacta (Fig. 3E). The less vascularized outermost cortical region possesses multiple (six) closely spaced LAGs (Fig. 3B). Below these LAGs, there is a band of two closely spaced LAGs, followed by an annulus toward the inner cortex (Fig. 3B). While this less vascularized outermost cortical region bears the hallmarks of an external fundamental system (EFS *sensu* Klein and Sander, 2008, Sander et al., 2011b), it is not completely avascular and most likely represents the beginning of an EFS.

The largest femur NMQR 1705/600 (885-mm length) also shows growth marks in the inner cortex, three LAGs are present in the mid-cortical region, followed by five more LAGs toward the outer cortical region. However, it lacks the modulation in vascular channels as seen in NMQR/1705/163, exhibiting the usual change from reticular to plexiform FLB from the inner to outer cortex.

In all femora with LAGs, there is a distinct lack of change in tissue type preceding and anteceding these growth lines in contrast to the zonal bone condition seen in less derived sauropodomorphs.

Detailed Histology of the Humeri

Growth lines in the form of LAGs are apparent throughout the cortex of the humeri, although apart from the actual lines there does not seem to be a change in the type of tissue abutting them. Humeri NMQR 1705/801 (570 mm preserved length) and 359 (620-mm length) do exhibit sparse secondary osteons in the perimedullary region, although humerus NMQR 1705/028 (which is intermediate in size between the two at 615 mm in length) does not.

Humeri NMQR/1705/801 and 359 show a change in vascular arrangement from reticular to plexiform from the inner to outer cortex. In NMQR/1705/801, sparse secondary osteons are present in the perimedullary region. Seven LAGs are evident toward the outer cortex, with the outer-most three being "double" LAGs, followed by a "triple" LAG, two closely spaced LAGs and approaching the inner cortical region a single LAG occurs (Fig. 4). These growth lines occur throughout the compacta, but there is no change in vascular arrangement (plexiform) of the surrounding FLB tissue.

The core sample from NMQR/1705/028 (Fig. 5) differs in that it is composed almost exclusively of plexiform FLB and lacks the change in orientation of FLB from reticular to plexiform seen in the other two humeri. There is however, a regional change to a less organized reticular arrangement of FLB midway up the cortex (Fig. 5A) and

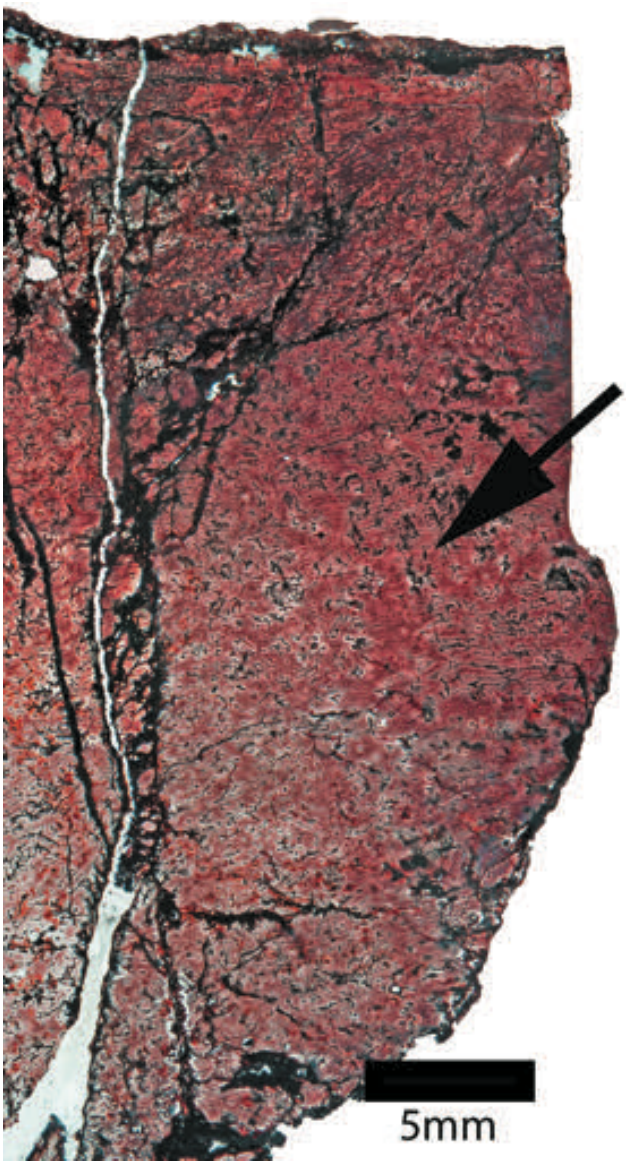

Fig. 2. Left femur, NMQR 1705/801. Isolated patch of plexiform FLB showing localized change in vascularization indicated by black arrow.

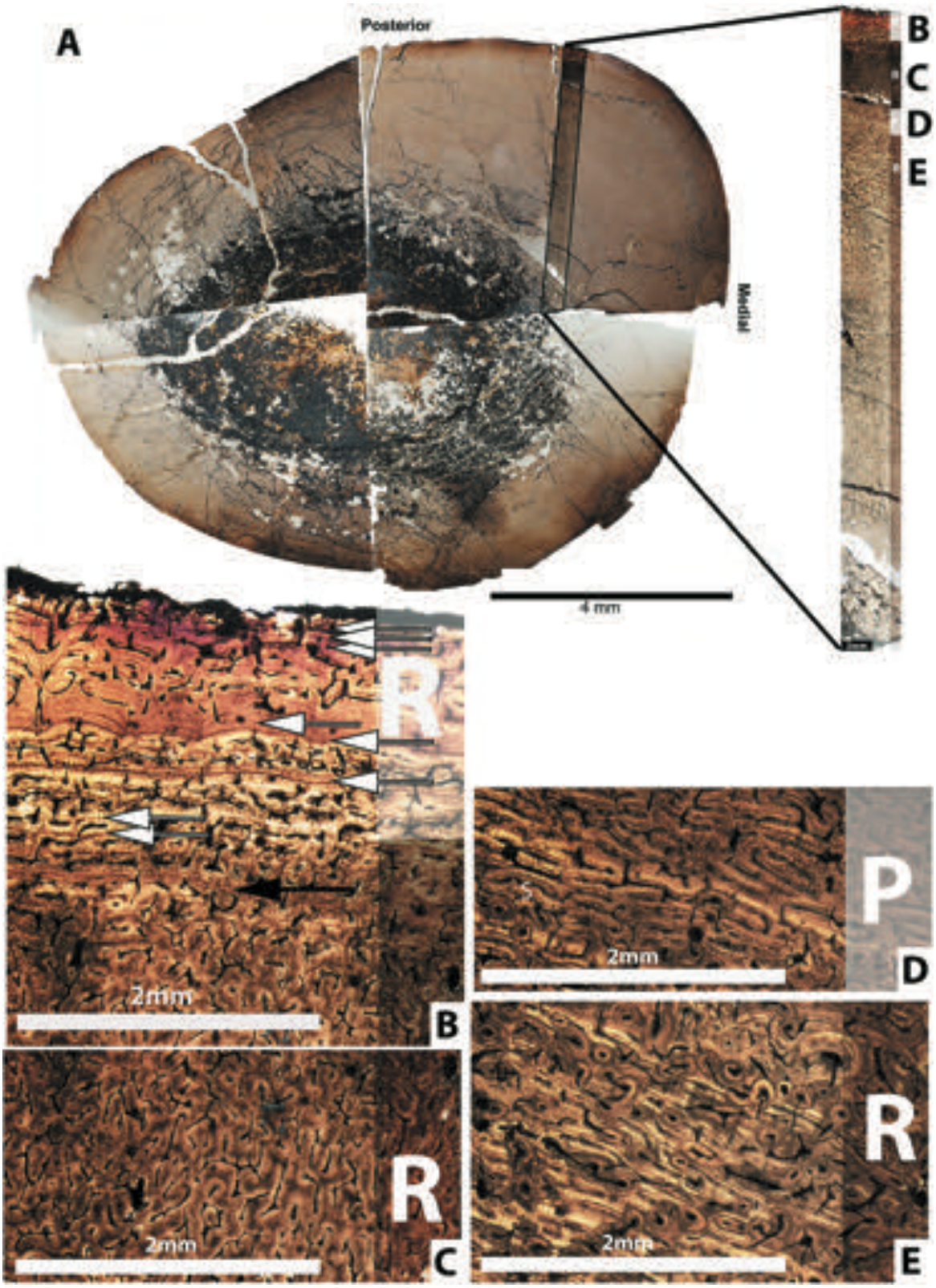

Fig. 3. Right femur, NMQR 1705/163 (**A**) view of overall cross-section. (**B**) Outermost cortical layer showing change from plexiform to reticular FLB, note reduction in vascularization and presence of eight LAGs (white arrows) and an annulus (black arrow) in outermost cortical margin. (**C**) Subsequent bone tissue below (B), showing continuation of reticular FLB. (**D**) Thin layer of plexiform FLB with some secondary osteons, (**E**) Innermost cortical region composed of reticular FLB with abundant secondary osteons. R, reticular FLB; P, plexiform FLB; S, secondary osteons.

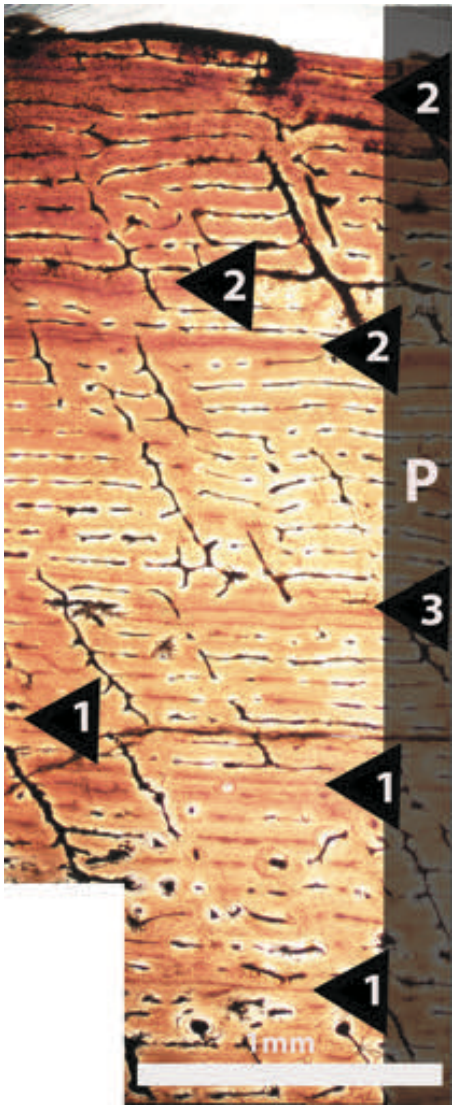

Fig. 4. Right humerus, NMQR 1705/801.Black triangles with numbers indicate occurrence and number of LAGs, that is, single, double, or triple LAGs. P, plexiform FLB.

again just below a thin band of radial FLB tissue just above the second innermost LAG (Fig. 5B). Above this radial band, there are three more closely spaced LAGs in the subperiosteal cortex (Fig. 5C). However, this outer region of the cortex does not exhibit a decrease in vascularization or change in the arrangement of FLB that would be considered an EFS (*sensu* Sander et al., 2011b). The band of localized radial FLB (Fig. 5B) is followed by the resumption of normal plexiform FLB. Secondary osteons are absent in this sample.

NMQR 1705/359 also exhibits growth lines in the form of seven LAGs approaching the outer cortex, five of which are closely spaced and are in the outermost fringe of the cortex, below these are two more closely spaced LAGs (Fig. 6). Note that these two LAGs are separated by a region of plexiform FLB, and thus, LAGs are not restricted only to the outermost cortical layer as in the more derived sauropods (Sander et al., 2004, 2011a).

Detailed Histology of the Tibiae

The histology of the tibia generally conforms to the pattern seen in the femora and humeri having FLB with a vascular change from reticular to plexiform toward the outer-most cortex. Sparse secondary osteons are present in the perimedullary region (Fig. 7B). The smallest element, NMQR 1705/304(322 mm preserved length), does not exhibit any growth lines and shows uninterrupted deposition of FLB. The perimedullary region exhibits a reticular arrangement of FLB, with no secondary osteons.

Tibia NMQR 1705/561 (Fig. 8) (445 mm preserved length) also exhibits exclusively FLB, but with a predominantly plexiform vascular arrangement. However, in the upper third of the cortex there is a band of radially oriented FLB (Fig. 8A) (similar to that observed in humerus NMQR 1705/028, Fig. 5B). Three LAGs are present in the innermost half of the cortex, followed by two closely spaced LAGs just below the band of radial FLB and, a single LAG above the radial FLB band followed by three closely spaced LAGs. As in NMQR 1705/028, resumption of normal growth occurs after the "event" that caused the radial deposition.

However, in Tibia NMQR 1705/235 (500-mm length) there is a divergence from the general pattern seen among the tibia. It is composed almost exclusively of plexiform FLB tissue, apart from a small region of reticular FLB just above the medullary region and two patches in the subperiosteal cortex. No growth marks are evident.

Among the two largest tibia NMQR 1705/354 and NMQR 1705/009 (565 mm as preserved), there is the characteristic change from reticular FLB in the perimedullary region to plexiform FLB toward the outer cortex. In the former, approaching the outer-most layer of the cortex there is a reduction in vascularization, five LAGs are present in this region. It is similar to femur NMQR 1705/163, in terms of the reduction in vascularization and predominance of LAGs in the outer-most cortical layers. However, in contrast NMQR 1705/009 exhibits three LAGs spanning the cortex.

DISCUSSION

General Histological Features

Samples taken from the midshaft femora, tibia, and humeri exclusively exhibit well vascularized, FLB tissue (see Table 1.). The organization of the vascular channels of the FLB is characterized by a reticular (irregular) arrangement in the inner cortex and a change in orientation to a more plexiform arrangement (laminar channels joined by radial anastomoses) toward the outer cortex (Fig. 7). Note however that this is a general trend and certain elements show combinations of reticular, plexiform, and radial tissue, as well as changes in the degree of vascularization in the outer cortical region. Primary osteons are present throughout the compacta and secondary osteons are present in the inner cortical regions of most bones, extending into the outer cortex in some (notably NMQR/1705/163). In femur NMQR/1705/163, Haversian reconstruction has progressed quite far, with several generations of secondary osteons present, however interstitial primary FLB is still present. In stark contrast, femur NMQR 1705/252 exhibits no secondary osteons, with sparse occurrences of enlarged channels from the mid-cortex inwards.

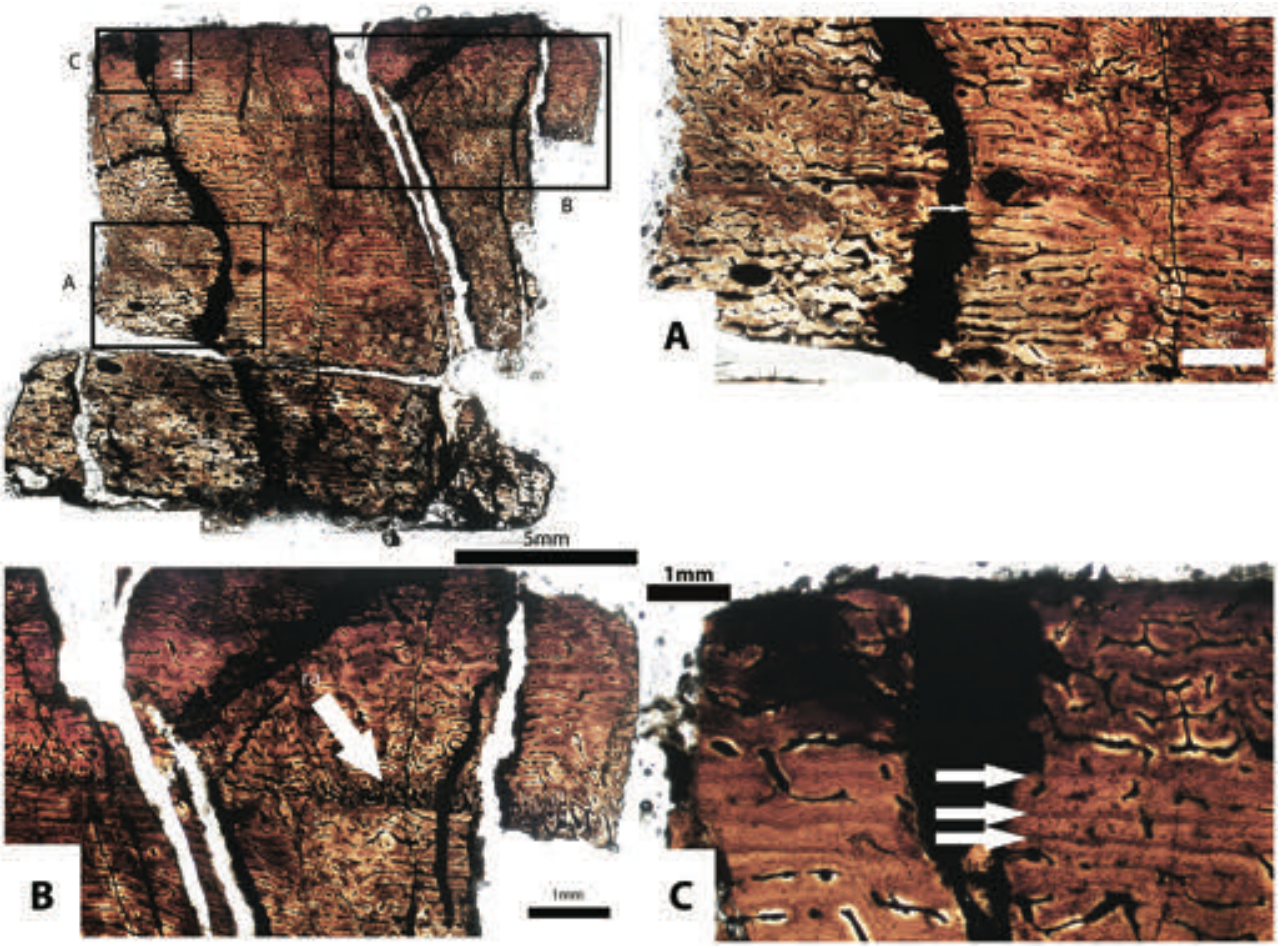

Fig. 5. Right humerus, NMQR 1705/028.Composed almost exclusively of FLB. (**A**) Mid-cortical area showing localized change to reticular FLB and LAG followed by annulus. (**B**) Band of radial FLB tissue. **C)** Outermost cortical region with band of three LAGs. Horizontal white and black arrows indicate LAGs and annuli. Ra, radial FLB; Re, reticular FLB.

Most of the long bones sampled show growth marks, which are predominately LAGs. Three femora (NMQR 1705/163, NMQR 1705/020, and BPI/1/4952) preserve annuli, while one humerus (NMQR 1705/028) preserves an annulus associated with a LAG. While a decrease in growth rate is apparent based on the reduction in vascularization (of the FLB tissue) and a concentration of LAGs in the subperiosteal margin of femur NMQR/1705/163 (Fig. 3A,B), LAGs are not restricted to this layer. Furthermore, there is no change in tissue type or vascular arrangement of the FLB immediately apical or basal to the growth lines in the inner compacta.

As with both the femora and humeri, generally the tibiae exhibit a change from reticular organization of the FLB to a plexiform arrangement toward the outer cortex. In the case of tibia NMQR 1705/235 (500-mm length), patches of reticular FLB are present in the subperiosteal cortex and there is no evidence of growth lines in the inner cortex. This contrasts with tibia NMQR 1705/354 (assumed to be from a juvenile based on length [322 mm]), which has almost exclusively plexiform bone tissue and exhibits at least five LAGs in the outer region of the cortex.

Among the femora, the smallest specimen (NMQR 1705/252 [435 mm]) shows no growth marks and is composed of uninterrupted FLB (see Fig. 9). However, there is a distinctive change in vascular orientation (modulation) from an earlier formed reticular bone to a later formed plexiform arrangement. The larger femora show a slight decrease in vascularization in the outermost part of the cortex. This less vascularized outermost cortical region is also characterized by a prevalence of LAGs.

Two of the humeri show the transition from reticular to plexiform FLB. However, humerus NMQR 1705/028 is composed almost exclusively of plexiform FLB with two patches (see Fig. 5) showing a regional change to reticular FLB. Furthermore, close to the peripheral edge, there is a thin band of radially oriented FLB which resembles the sunburst pattern typical of periosteal reactive growth (Chinsamy and Tumarkin-Deratzian, 2009). A similar band of radial FLB is also present in tibia NMQR 1705/561. In both elements, the radial FLB is followed by normal bone deposition.

When comparing similar sized humeri, femora, and tibiae, all are composed of FLB, with most showing modulations in vascular organization from reticular to plexiform FLB (for exceptions to this pattern see Table 1). The presence of secondary osteons in similar sized elements is apparent in femora and tibia. However, in the humeri

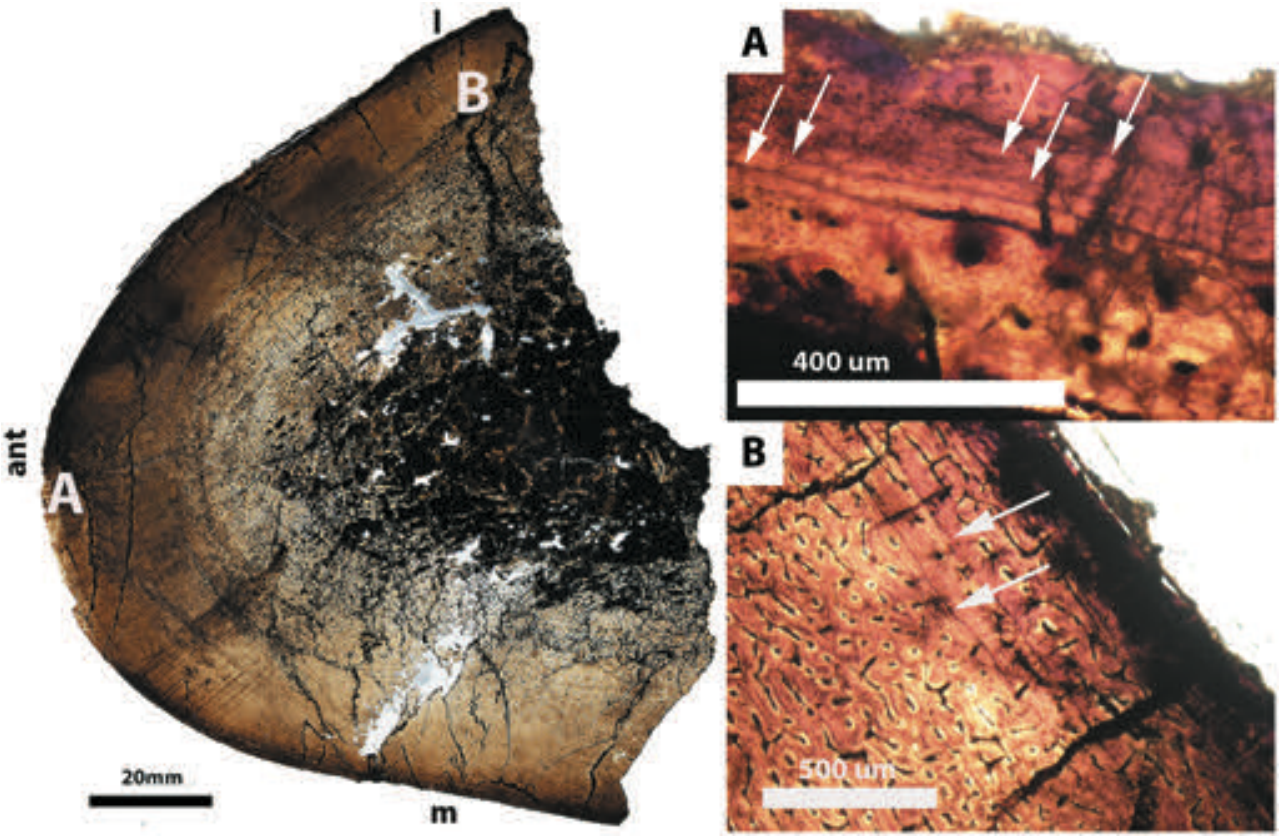

Fig. 6. Left humerus, NMQR 1705/359. (**A**) Outer-most cortical margin showing five closely spaced LAGs (white arrows), (**B**) Two closely spaced LAGs (white arrows) deeper in the cortex. The edge of the bone is not the periosteal surface, which has flaked off. Ant, anterior; l, lateral; m, medial.

this is not the case, as humerus NMQR 1705/359 and NMQR 1705/028 are almost the same length (620 mm and 615 mm, respectively)—yet secondary osteons are present in the former but not the latter. In terms of growth marks, there appears to be a large degree of variability in their occurrence among similar sized elements.

Growth Dynamics

Ontogenetic changes in the growth dynamics of *Antetonitrus* are evident based on the specimens studied. Early in ontogeny (as seen in femur NMQR 1705/252 and tibia NMQR 1705/304) it appears that *Antetonitrus* was characterized by rapid, uninterrupted growth, with deposition of reticular FLB, followed by a textural shift to plexiform FLB midway up the cortex. There is a total lack of growth marks or secondary osteons in these individuals. There is a large jump in size from these smallest elements (510 mm and 322 mm, respectively) to the next longest complete elements in the sample of 256 mm in the femora and 178 mm in the tibia. While the larger bones are still composed of FLB and possess the textural shift from reticular to plexiform FLB these bones show evidence of intermittent growth marks throughout the cortex, as well as evidence of secondary remodeling. However, except for femur NMQR 1705/163 there is no evidence of termination of growth in the external cortex of the other bones yet, indicating that they are sub-adult. In femur NMQR 1705/163, a gradual decrease in vascularization is evident in the outer cortical layer indicating that bone depositional rate had slowed down; however, this region is not completely avascular. There is also a concentration of LAGs in this less well vascularized outer cortical region. This may correspond to the beginning of an EFS (*sensu* Klein and Sander, 2008). If this is the case, then *Antetonitrus* would have possessed a determinant growth strategy.

Based on bone length there is no association between size and number of growth lines (see Table 1), with larger individuals possessing fewer growth marks than smaller individuals in some cases: NMQR 1705/163 is the oldest femora based on growth marks and has an incipient EFS, but in terms of length, it is only the 5th largest femur. Considering the humeri, NMQR 1705/801 exhibits the most growth marks, despite being the smallest humerus. These findings suggest that the size of the element is not a good proxy for age. These findings suggest intra-specific differences that could be due to sexual dimorphism (which cannot be tested as the sample is too small) or perhaps to developmental plasticity as described for *Plateosaurus* (Sander and Klein, 2005). A third possibility is that these LAGs could represent random periods of resource limitation similar to those occurring in large mammals seasonally (Köhler and Moyà-Solà, 2009; Köhler et al., 2012), although there is no published data to suggest that these occur non-annually.

In contrast to the dichotomy proposed by Sander et al. (2004) between growth patterns for basal Sauropodomorpha and Sauropoda, it appears that at least in

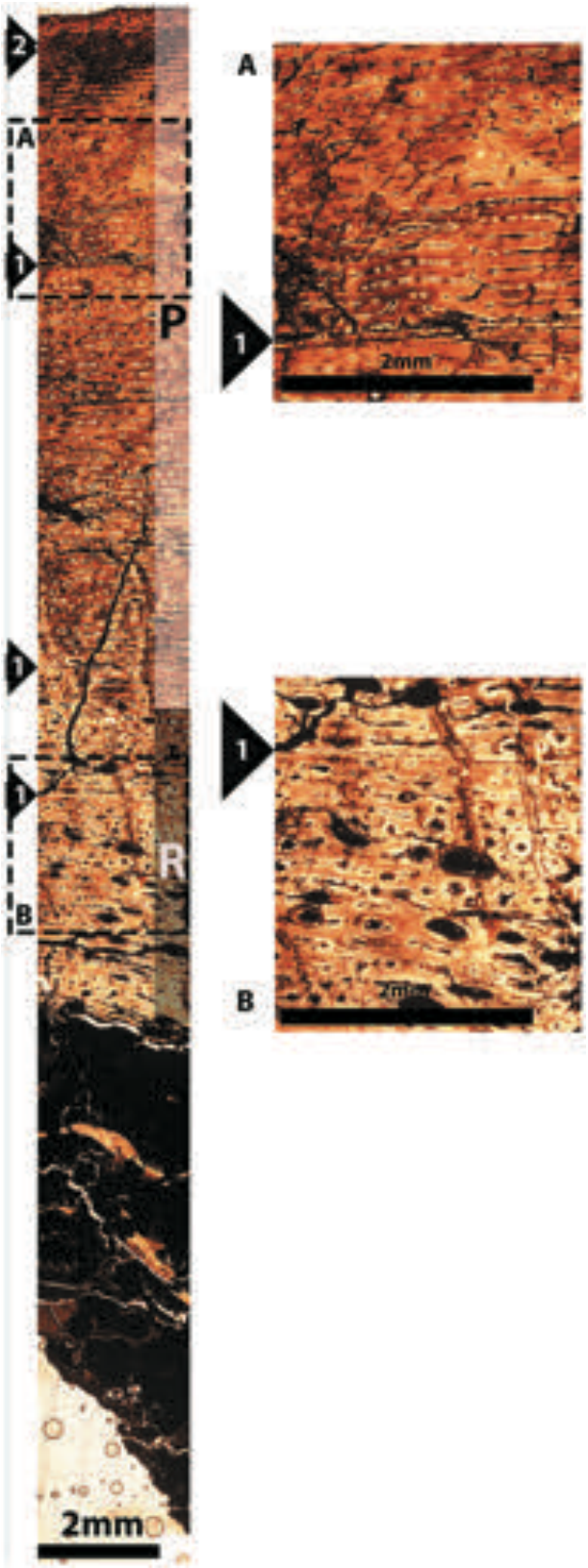

Fig. 7. Right tibia, NMQR 1705/009. Textural shift from reticular (**A**) to plexiform (**B**) FLB. Black triangles with numbers indicate occurrence and amount of closely spaced LAGs, that is, single or double LAGs. R, reticular; P, plexiform.

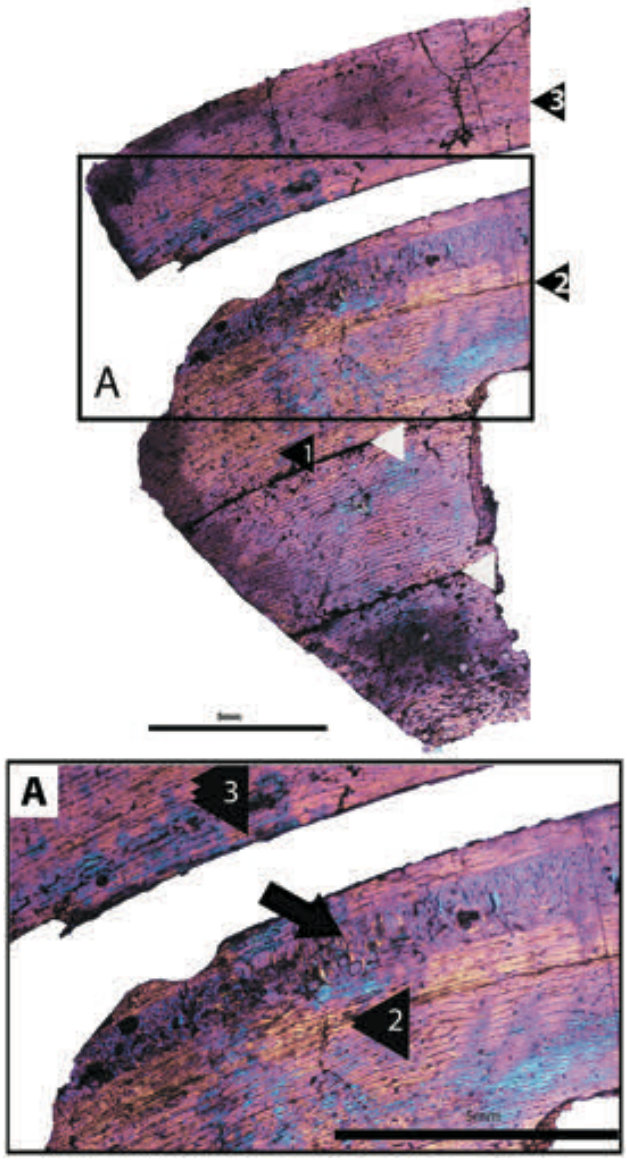

Fig. 8. Right tibia, NMQR 1705/561. Polarized Light. Note preponderance of plexiform FLB. (**A**) Region with band of radial FLB indicated by black arrow. Black triangles indicate LAGs; arrowheads indicate LAGs, and the numbers indicate single, double, or triple LAGs. White triangles indicate fractures that may correspond to LAGs. ra, radial FLB.

early sauropods like *Antetonitrus*, growth lines are not restricted to the outer cortical layer and occur throughout ontogeny, albeit irregularly. Despite this, highly vascularized FLB predominates in the cortex—as in the Tendaguru neosauropods (Sander, 2000; Sander et al., 2004, 2011a). One femur (NMQR 1705/163) shows a reduction in vascularization and concentration of LAGs in the outermost cortical layer, suggesting that its growth was slowing down or had virtually stopped. While growth marks occur throughout the cortex of most bones sampled, it should be noted that there is no associated change in degree or pattern of vascularization prior to or after the growth marks in contrast to *Lessemsaurus* (Cerda et al., 2017).

TABLE 1. List of specimens studied, including summary of histological features

Accession No.	Element	Length (mm)	Sample location	Primary bone	Growth marks	Bone tissue from medullary region to peripheral edge	Secondary osteons	Dense Haversian bone	Maximum cortical thickness from midshaft segment sampled (mm)
NMQR 1705/252	F	435[a,b]	Posteromedial	Fibrolamellar	-	Re, P	No	No	17.04
NMQR 1705/020	F	756	Posteromedial	Fibrolamellar	3,? Annulus	Re, P	Yes	No	43.13
NMQR 1705/801	F	760	Posteromedial	Fibrolamellar	No	Re	Yes	No	43.13
NMQR 1705/163	F	770	Cross-section, Posteromedial	Fibrolamellar	8 LAGS, Annulus	Re, P, Re, P	Yes	Incipient	44.00
BPI/1/4952a	F	770	Posterior	Fibrolamellar	Annulus, 3 LAGS	Re	No	No	20.00
NMQR 1705/325	F	793	Posteromedial	Fibrolamellar	2 LAGs	Re, P	Yes	No	31.48
NMQR 1705/15	F	795	Posteromedial	Fibrolamellar	No	Re,P	Yes	No	41.19
NMQR 1705/600	F	885	Posteromedial	Fibrolamellar	Yes, 5 LAGs	Re,P	Yes	No	41.10
NMQR 1705/801	H	570[a]	Anterolateral	Fibrolamellar	Yes, 7 LAGs	Re,P	Yes	No	26.15
NMQR 1705/359	H	620	Anterolateral	Fibrolamellar	Yes, 7 LAGs	Re,P	Yes	No	17.97
NMQR 1705/028	H	615	Anterolateral	Fibrolamellar	Yes, 5 LAGs, Annulus	P, Ra, P	No	No	14.10
NMQR 1705/304	T	322[a]	Anteromedial	Fibrolamellar	No	Re, P	No	No	15.47
NMQR 1705/561	T	445[a]	Posteromedial	Fibrolamellar	Yes, 6 LAGs	P, Ra, P	No	No	21.56
NMQR 1705/235	T	500	Posterior	Fibrolamellar	No	Re, P	No	No	22.55
NMQR 1705/100	T	520[a]	Posteromedial	Fibrolamellar	Yes, 2 LAGs	Re, P	Yes	No	23.22
NMQR 1705/354	T	565[a]	Posteromedial	Fibrolamellar	Yes, 5 LAGS	Re, P	Yes	No	23.23
NMQR 1705/009	T	565	Posteromedial	Fibrolamellar	Yes, 4 LAGS	Re, P	Yes	No	21.49

[a]Indicates incomplete/damaged bones.
[b]While the proximal end of left femur NMQR 1705/252 is incomplete, the corresponding complete right femur NMQR 1705/304A is complete and its length of 510 mm will be used in size comparisons.
F, femur; H, humerus; T, tibia; Re, reticular; P, plexiform; Ra, Radial.

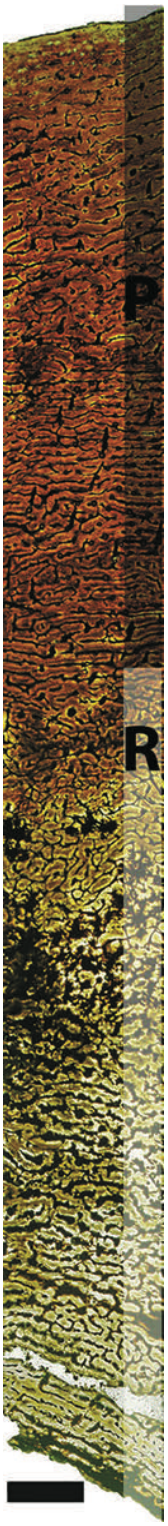

Fig. 9. Left femur, NMQR 1705/252. Juvenile individual exhibiting uninterrupted FLB throughout the cortex. Note the lack of growth marks and secondary osteons. Note the textural shifts in FLB. P, plexiform FLB; R, reticular FLB.

The majority of the *Antetonitrus* bones also show modulations between reticular and plexiform FLB. This feature is also seen in the femoral histology of *Lessemsaurus* and *Volkheimeria* (Cerda et al., 2017). Such textural shifts (*sensu* Chinsamy et al., 2012) are reminiscent of those seen in temperate populations of *Edmontosaurus* and *Hypacrosaurus* (Chinsamy et al., 2012), reflecting periodic strains in resource acquisition. The lack of consistent cycles of vascular modulation in NMQR 1705 precludes seasonality as a factor and is more similar to the inconsistent changes seen in temperate *Edmontosaurus* populations (Chinsamy et al., 2012). In most samples, there is only one textural shift from reticular to plexiform FLB tissue that occurs approximately halfway up the cortex. This may be evidence of a dietary change during ontogeny but fails to explain the multiple textural shifts seen in the femur NMQR 1705/163, a feature which is also present in *Lessemsaurus* and *Volkheimeria* (Cerda et al., 2017). Based on the number of LAGs (eight) and the reduction in vascularization in the outermost cortical layer of femur NMQR 1705/163 indicating that this femur belonged to the oldest individual, it seems more likely that multiple textural shifts are a function of increased age.

Phylogenetic Context

When looking a range of sauropodomorphs spanning, the transition from basal forms (i.e., *Massospondylus* and *Plateosaurus*), to more derived sauropodiforms (i.e., *Aardonyx*, *Leonerasaurus*, and *Mussaurus*) to the most basal sauropod—*Antetonitrus*, there is a trend toward an increase in the deposition of highly vascularized FLB as the predominant cortical bone tissue. This trend starts with *Mussaurus* (see Cerda et al., 2014, 2017) and appears to continue in *Antetonitrus.*

Based on the juvenile material of *Antetonitrus* studied here and the juvenile *Mussaurus* material (Cerda et al., 2014), it appears that both taxa exhibited a phase of early uninterrupted rapid growth. The presence of growth marks in the outer cortical layers of adult *Mussaurus* specimens, may indicate that both taxa exhibited growth marks later in ontogeny after this rapid phase of growth, followed by a reduction in vascularization and preponderance of growth marks in the outermost cortical layer (based on femur NMQR 1705/163), which likely correspond to an external fundamental system (*sensu* Klein and Sander, 2008). The similarity between the two species growth dynamics show remarkable convergence. However, Cerda et al. (2017) hypothesize that the most parsimonious explanation for the occurrence of similar growth strategies in the basal sauropodiform, *Mussaurus* and in more derived sauropods is due to homoplastic convergence.

In *Antetonitrus*, the absence of growth marks in the inner cortex seen in more derived neosauropod taxa (Curry, 1999; Sander, 2000; Sander et al., 2004, 2011a) and *Mussaurus* (Cerda et al., 2017) is lacking, however this may be due to the material under study belonging to sub-adult individuals.

Occurrence of Radial Fibrolamellar Tissue and Pathology

The presence of radial FLB in the cortical region of a humerus and tibia may be periosteal reactive bone, indicative of pathological growth (Chinsamy and Tumarkin-

Deratzian 2009). In the latter study, radial spicules radiated from the periosteal and endosteal margins of the bones. In contrast, the humerus and tibia belonging to NMQR 1705 the band of radial FLB is located within the cortex, indicating that after a period of trauma/illness, normal growth resumed. This pattern (and the lack of evidence of endosteal deposits) is more similar to that reported in *Psittacosaurus mongoliensis*, *Plateosaurus engelhardti*, and a Late Triassic dinosaur from Norway (Chinsamy et al., 2012), and may be related to hypertrophic osteopathy (see Lenehan and Fetter, 1985; Chinsamy et al., 2012). The ratio of the length of the humerus to tibia in the *Antetonitrus* holotype (BPI/1/4952) is 1.33, and for NMQR 1705 the humerus (NMQR 1705/028) and incomplete tibia (NMQR/1705/561) the ratio is 1.38. As the length of the incomplete tibia is approximated, it is possible that the ratio would be less in reality. Given that both the aforementioned humerus and tibia of NMQR 1705 possess five LAGs each, and both have the anomalous radial fibrolamellar bone in the outermost part of their cortices, it is possible that these bones are from the same individual (see Sander, 2000). In lieu of other data on association between elements belonging to NMQR 1705, this is tentative proof that NMQR 1705/028 and NMQR 1705/561 belong to the same individual.

CONCLUSION

It appears that the growth strategies present in the earliest member of Sauropoda (*sensu* Yates, 2007) are not a continuation of patterns first seen in the basal sauropodiform, *Mussaurus*, which are similar to more derived sauropods. This means that uninterrupted deposition of highly vascularized FLB coupled with restriction of growth marks to the outer cortical margins is not a synapomorphy for Sauropodiformes. The presence of the "typical" sauropod growth pattern in both *Mussaurus* and derived sauropods, yet absence in *Antetonitrus* and *Lessemsaurus* suggests that the similarities between *Mussaurus* and more derived Sauropoda are the result of convergent evolution (see Cerda et al., 2017).

While there is an increase in the deposition of highly vascularized FLB in the cortex relative to basal sauropodomorphs, both *Antetonitrus* and *Lessemsaurus* exhibit evidence of growth marks throughout the compacta—although less regularly in *Antetonitrus*. Cerda et al. (2017) show that the basal sauropods *Lessemsaurus*, *Volkheimeria*, and *Patagosaurus* exhibit subtle differences in growth patterns: cyclical growth in *Lessemsaurus* (reminiscent of basal sauropodomorphs) with marked textural shifts, poorly defined textural shifts in FLB in *Volkheimeria* and poorly formed annuli interspersing the FLB in *Patagosaurus* (Cerda et al., 2017). Compared to these three taxa, *Antetonitrus* appears to possess growth lines (although not quite as cyclical) and textural shifts as in *Lessemsaurus* (and to a lesser extent *Volkheimeria*).

However, ultimately *Antetonitrus* shows a unique bone depositional pattern. One unsurprisingly similar to its sister-taxon (*Lessemsaurus*)—but different in two key ways: (1) the regularity and cyclical frequency of growth marks in the cortex, and (2) lack of textural shifts from reticular to plexiform FLB presaging LAGs. Thus, changes in growth dynamics seen *en route* to Sauropoda appear to be confounded by homoplasy and high levels of plasticity. In the case of *Antetonitrus*, this suggests that there is no discrete "Sauropod pattern" in terms of growth dynamics and that changes in growth from basal sauropodomorphs to derived sauropods does not occur along a continuum.

Despite this, *Antetonitrus* appears to follow the general trend, as seen in Sauropoda, of a rapid increase in growth rates during early ontogeny (as evidenced by the deposition of uninterrupted FLB). Termination of growth was not recorded, but one specimen exhibited a slowdown in growth in the outermost cortex (i.e., the beginning of an EFS)—indicating that we may still be dealing with somatically immature individuals. Furthermore, our study shows that the developmental plasticity seen in basal sauropodomorphs such as *Plateosaurus* is still present in more derived forms such as *Antetonitrus*. Infrequent modulations in vascularization patterns indicate that the animals studied probably experienced periods of environmental stress (e.g., food shortages), although not on a regular, seasonal basis.

We propose that further histological studies on the immediate outgroup to Sauropoda (i.e., *Melanorosaurus*), the basal sauropod *Blikanasaurus cromptoni* (Galton and Van Heerden, 1998), the non-eusauropod sauropod taxa *Gonxianosaurus shibeinsis* (He *et al*., 1998), and *Tazoudasaurus naimi* (Allain et al., 2004) will provide a more complete assessment of the changes in growth strategies during the transition from more basal sauropodiforms to true sauropods.

ACKNOWLEDGMENTS

The authors are grateful to J. Botha-Brink and E. Butler (National Museum, Bloemfontein, South Africa) for allowing for the histological analysis of NMQR 1705; as well as B. Rubidge and B. Zipfel (Evolutionary Studies Institute, Johannesburg, South Africa) for access to the holotype of *Antetonitrus ingenipes* and other comparative material on countless occasions. We thank Ignacio Cerda (Universidad Nacional de Río Negro, Rio Negro, Argentina) and two anonymous reviewers for constructive criticism that improved this manuscript. This work was supported by a South African National Research Foundation (NRF) Scarce Skills Bursary and Paleontological and Scientific Trust (PAST) grant to E. Krupandan.

LITERATURE CITED

Allain R, Aquesbi N, Dejax J, Meyer C, Monbaron M, Montenat C, Richir P, Rochdy M, Russell D, Taquet P. 2004. A basal sauropod dinosaur from the Early Jurassic of Morocco. C R Palevol 3: 199–208.

Apaldetti C, Pol D, Yates A. 2013. The postcranial anatomy of *Coloradisaurus brevis* (Dinosauria: Sauropodomorpha) from the late Triassic of Argentina and its phylogenetic implications. Palaeontology 56:277–301.

Bordy EM, Van Gen J, Tucker R, McPhee BW. 2015. Maphutseng fossil heritage: Stratigraphic context of the dinosaur trackways and bone bed in the Upper Triassic–Lower Jurassic Elliot Formation (Karoo Supergroup, Lesotho). Proc Abstr/I Int Congr Contl Ichnol 1:67.

Buffetaut E, Suteethorn V, Cuny G, Tong H, Le Loeuff J, Khansubha S, Jongautchariyakul S. 2000. The earliest known sauropod dinosaur. Nature 407:72–74.

Buffetaut E, Suteethorn V, Le Loeuff J, Cuny G, Tong H, Khansubha S. 2002. The first giant dinosaurs: A large sauropod from the Late Triassic of Thailand. C R Palevol 1:103–109.

Cerda IA, Pol D, Chinsamy A. 2013. Osteohistological insight into the early stages of growth in *Mussaurus patagonicus* (Dinosauria, Sauropodomorpha). Hist Biol 26:110–121.

Cerda IA, Chinsamy A, Pol D. 2014. Unusual endosteally formed bone tissue in a Patagonian basal sauropodomorph dinosaur. Anat Rec 297:1385–1391.

Cerda I, Chinsamy A, Pol D, Apaldetti C, Otero A, Powell J, Martinez R. 2017. Novel insight into the origin of the growth dynamics of sauropod dinosaurs, and the attainment of gigantism. PLoS One 12:e0179707.

Charig AJ, Attridge J, Crompton AW. 1965. On the origin of the sauropods and the classification of the Saurischia. Proc Linn Soc Lond 176:197–221.

Chinsamy A, Raath MA. 1992. Preparation of fossil bone for histological examination. Palaeont Afr 29:39–44.

Chinsamy A. 1993a. Image analysis and the physiological implications of the vascularization of femora in archosaurs. Mod Geol 19: 101–108.

Chinsamy A. 1993b. Bone histology and growth trajectory of the prosauropod dinosaur *Massospondylus carinatus* Owen. Mod Geol 18: 319–329.

Chinsamy A. 1994. Dinosaur bone histology: Implications and inferences. Paleont Soc Spec Pub 7:213–227.

Chinsamy A, Tumarkin-Deratzian A. 2009. Pathologic bone tissues in a turkey vulture and a nonavian dinosaur: Implications for interpreting endosteal bone and radial fibrolamellar bone in fossil dinosaurs. Anat Rec 292:1478–1484.

Chinsamy A, Thomas DB, Tumarkin-Deratzian AR, Fiorillo AR. 2012. Hadrosaurs were perennial polar residents. Anat Rec 295: 610–614.

Chinsamy-Turan A. 2005. *The microstructure of dinosaur bone*. Baltimore, MD: Johns Hopkins University Press.

Curry KA. 1999. Ontogenetic histology of *Apatosaurus* (Dinosauria: Sauropoda): New insights on growth rates and longevity. J Vert Paleont 19:654–665.

Curry Rogers K, Whitney M, D'Emic M, Bagley B. 2016. Precocity in a tiny titanosaur from the Cretaceous of Madagascar. Science 352: 450–453.

De Ricqlès A. 1983. Cyclical growth in the long limb bones of a sauropod dinosaur. Acta Palaeontol Pol 28(1–2):225–232.

Ellenberger F, Ellenberger P. 1956. Le gisement de Dinosauriens de Maphutseng. C R Soc Géol Fr 8:99–101.

Galton PM, Van Heerden J. 1998. Anatomy of the prosauropod dinosaur *Blikanasaurus cromptoni* (Upper Triassic, South Africa), with notes on the other tetrapods from the lower Elliot Formation. J Paläontol Z 72:163–177.

Gauffre F-X. 1993. Biochronostratigraphy of the lower Elliot Formation (Southern Africa), and preliminary results on the Maphutseng dinosaur (Saurischia: Prosauropoda) from the same formation of Lesotho. Bull N M Mus Nat Hist Sci 3:147–149.

He X, Wang C, Liu S, Zhou F, Lui T, Cai K, Dai B. 1998. A new species of sauropod from the early Jurassic of Gongxian co., Sichuan. Acta Geol Sich 18:1–7.

Hurum JH, Bergan M, Muller R, Nystuen JP, Klein N. 2006. A Late Triassic dinosaur bone, offshore Norway. Norsk Geol Tidsskr 86:117.

Klein N, Sander PM. 2007. Bone histology and growth of the prosauropod dinosaur *Plateosaurus engelhardti* Von Meyer, 1837 from the Norian bonebeds of Trossingen (Germany) and Frick (Switzerland). Spec Pap Palaeontol 77:169.

Klein N, Sander PM. 2008. Ontogenetic stages in the long bone histology of sauropod dinosaurs. Paleobiology 34:247–263.

Köhler M, Moyà-Solà S. 2009. Physiological and life history strategies of a fossil large mammal in a resource-limited environment. Proc Natl Acad Sci USA 106:20354–20358.

Köhler M, Marín-Moratalla N, Jordana X, Aanes R. 2012. Seasonal bone growth and physiology in endotherms shed light on dinosaur physiology. Nature 487:358–361.

Lehman TM, Woodward HN. 2008. Modeling growth rates for sauropod dinosaurs. Paleobiology 34:264–281.

Lenehan TM, Fetter AW. 1985. Hypertrophic osteodystrophy. In: Newton CD, Nunamaker DM, editors. *Textbook of small animal orthopedics*. Baltimore, MD: Lippincott. p 597.

Mannion PD. 2010. A revision of the sauropod dinosaur genus '*Bothriospondylus*' with a redescription of the type material of the Middle Jurassic form '*B. madagascariensis*'. Palaeontology 53:277–296.

McPhee BW, Yates AM, Choiniere JN, Abdala F. 2014. The complete anatomy and phylogenetic relationships of *Antetonitrus ingenipes* (Sauropodiformes, Dinosauria): Implications for the origins of Sauropoda. Zool J Linn Soc 171:151–205.

Otero A, Pol D. 2013. Postcranial anatomy and phylogenetic relationships of *Mussaurus patagonicus* (Dinosauria, Sauropodomorpha). J Vert Paleont 33:1138–1168.

Pol D, Garrido A, Cerda IA. 2011. A new sauropodomorph dinosaur from the Early Jurassic of Patagonia and the origin and evolution of the sauropod-type sacrum. PLoS One 6:e14572.

Reid R. 1981. Lamellar-zonal bone with zones and annuli in the pelvis of a sauropod dinosaur. Nature 292:49–51.

Rimblot-Baly F, de Ricqlès A, Zylberberg L. 1995. Analyse paléohistologique d'une série de croissance partielle chez *Lapparentosaurus madagascariensis* (Jurassique Moyen): Essai sur la dynamique de croissance d'un dinosaure sauropode. Annls Paléont (Vert) 81:49–86.

Sander PM. 2000. Longbone histology of the Tendaguru sauropods: Implications for growth and biology. Paleobiology 26:466–488.

Sander PM, Klein N, Buffetaut E, Cuny G, Suteethorn V, Le Loeuff J. 2004. Adaptive radiation in sauropod dinosaurs: Bone histology indicates rapid evolution of giant body size through acceleration. Org Divers Evol 4:165–173.

Sander PM, Klein N. 2005. Developmental plasticity in the life history of a prosauropod dinosaur. Science 310:1800–1802.

Stein K, Sander PM. 2009. Histological core drilling: A less destructive method for studying bone histology. In: Brown MA, Kane JF, Parker WG, editors. *Methods in fossil preparation: proceedings of the first annual fossil preparation and collections symposium*. Petrified Forest: University of Nebraska. p 69–80.

Sander PM, Klein N, Stein K, Wings O. 2011a. Sauropod bone histology and its implications for sauropod biology. In: Gee CT, Klein N, Remes C, Sander PM, editors. *Biology of the sauropod dinosaurs: Understanding the life of giants*. Bloomington, IN: Indian University Press. p 276–302.

Sander PM, Christian A, Clauss M, Fechner R, Gee CT, Griebeler E, Gunga H, Hummel J, Mallison H, Perry SF. 2011b. Biology of the sauropod dinosaurs: The evolution of gigantism. Biol Rev Camb Philos Soc 86:117–155.

Yates AM, Kitching JW. 2003. The earliest known sauropod dinosaur and the first steps towards sauropod locomotion. Proc R Soc B 270: 1753–1758.

Yates AM. 2007. The first complete skull of the Triassic dinosaur *Melanorosaurus* Haughton (Sauropodomorpha: Anchisauria). Spec Pap Palaeontol 77:9–55.

Yates AM, Bonnan MF, Neveling J, Chinsamy A, Blackbeard MG. 2010. A new transitional sauropodomorph dinosaur from the Early Jurassic of South Africa and the evolution of sauropod feeding and quadrupedalism. Proc R Soc B 277:787–794.